Effect of lattice distortion on uranium magnetic moments in $U_4Ru_7Ge_6$ studied by polarized neutron diffraction

Michal Vališka,[1,2,*] Milan Klicpera,[1] Petr Doležal,[1] Oscar Fabelo,[2] Anne Stunault,[2] Martin Diviš,[1] and Vladimír Sechovský[1]
[1]*Faculty of Mathematics and Physics, Charles University, DCMP, Ke Karlovu 5, CZ-12116 Praha 2, Czech Republic*
[2]*Institut Laue Langevin, 71 Avenue des Martyrs, CS 20156, F-38042 Grenoble Cedex 9, France*

(Received 21 November 2017; revised manuscript received 2 February 2018; published 16 March 2018)

In a cubic ferromagnet, small spontaneous lattice distortions are expected below the Curie temperature, but the phenomenon is usually neglected. This study focuses on such an effect in the $U_4Ru_7Ge_6$ compound. Based on DFT calculations, we propose a lattice distortion from the cubic Im-$3m$ space group to a lower, rhombohedral, symmetry described by the R-$3m$ space group. The strong spin-orbit coupling of the uranium ions plays an essential role in lowering the symmetry, giving rise to two different U sites (U1 and U2). Using polarized neutron diffraction in applied magnetic fields of 1 and 9 T in the ordered state (1.9 K) and in the paramagnetic state (20 K), we bring convincing experimental evidence of this splitting of the U sites, with different magnetic moments. The data have been analyzed both by maximum entropy calculations and by a direct fit in the dipolar approximation. In the ordered phase, the μ_L/μ_S ratio of the orbital and spin moments on the U2 site is remarkably lower than for the free U^{3+} or U^{4+} ion, which points to a strong hybridization of the U $5f$ wave functions with the $4d$ wave functions of the surrounding Ru. On the U1 site, the μ_L/μ_S ratio exhibits an unexpectedly low value: the orbital moment is almost quenched, like in metallic α-uranium. As a further evidence of the $5f$-$4d$ hybridization in the $U_4Ru_7Ge_6$ system, we observe the absence of a magnetic moment on the Ru1 site, but a rather large induced moment on the Ru2 site, which is in closer coordination with both U positions. Very similar results are obtained at 20 K in the ferromagnetic regime induced by the magnetic field of 9 T. This shows that applying a strong magnetic field above the Curie temperature also leads to the splitting of the uranium sites, which further demonstrates the intimate coupling of the magnetic ordering and structural distortion. We propose that the difference between the magnetic moment on the U1 and U2 sites results from the strong spin-orbit interaction with different local point symmetries.

DOI: 10.1103/PhysRevB.97.125128

I. INTRODUCTION

In condensed matter, the uranium $5f$ wave functions have a large spatial extent and interact strongly with the outer electrons of the neighboring ions leading to the loss of their atomic character and the delocalization of the $5f$ electrons. The outer-electron configuration of the ligands of a U ion, the coordination number, and the ligand sphere geometry hence play key roles in the physics of U intermetallics. The interplay between these physical characteristics gives a rise to an abundance of exotic physical phenomena often connected with complex $5f$ electron magnetism and various exotic low-temperature states. The loss of atomic character of the $5f$ electron wave functions and delocalization of $5f$ electrons have a fatal impact on the formation of the U magnetic moments, which are then often found dramatically reduced with respect to the U^{3+} and U^{4+} free-ion moment values. Unlike the $3d$ transition metals, which generally exhibit only a spin magnetic moment due to "freezing" of the orbital component in the crystal field, the relativistic effects, namely the strong spin-orbit interaction, in the heavy atoms like U induce a large orbital polarization [1,2], which is boosting the formation of a considerable orbital moment even in the case of itinerant $5f$ electrons. The relativistic energy band calculations performed for U compounds by rule provide an orbital component larger than the antiparallel spin component of a U magnetic moment [1–7]. These findings are in agreement with the results of polarized neutron diffraction (PND) studies of U compounds. The pioneering PND studies were focused on US [8], UO_2 [9,10], and USb [11], considered to be localized $5f$ electron systems. The e-e interactions of U ions with ligands lead to a significant hybridization of the U $5f$-electron states with the non-$5f$ valence electron states ($5f$-ligand hybridization). A strong evidence of the important role of the $5f$-ligand hybridization was first experimentally revealed by PND on URh_3 [12] with the observation of the enhanced elemental susceptibility of the Rh ion, twice the value of metal Rh. The $5f$-ligand hybridization mechanism was theoretically explained for UT_3 and UX_3 (T = transition metal and $X = p$ element, respectively) compounds by Koelling *et al.* [13] and corroborated by band structure calculations performed by Eriksson *et al.* [14].

The delocalization of the $5f$ electrons due to the large overlap of the $5f$ wave functions of neighboring U ions and the strong $5f$-ligand hybridization is accompanied by a reduction of the $5f$ magnetic moment. Despite this, the strong spin-orbit coupling induces a predominant orbital magnetic moment antiparallel to the spin moment in the spin-polarized $5f$ energy bands as first demonstrated for the itinerant ferromagnet UN

*michal.valiska@gmail.com

[1]. This may lead to a very small total U magnetic moment, no more than a few hundredths of μ_B, as observed in the itinerant $5f$ ferromagnet UNi_2 [15], and further confirmed by polarized neutrons [16], and first-principles electronic structure calculations [5]. Despite the itinerant character of the magnetism, UNi_2 exhibits very strong magnetocrystalline anisotropy with $H_a \gg 35$ T at 4.2 K [5].

The most prominent example of almost complete compensation of the spin (μ_S) and orbital (μ_L) $5f$ moments is UFe_2 with $\mu_L = 0.23\,\mu_B$ and $\mu_S = 0.22\,\mu_B$, resulting in a net moment at the U site of only $0.01\,\mu_B$. This specific situation together with the considerably different spatial distributions of the orbital and spin magnetizations result in an unusual magnetic form factor exhibiting a maximum at a finite q [17,18]. The experimental observations fulfilled the theoretical prediction of Brooks *et al.* [19] based on the finding that the $5f$-ligand hybridization reduces disproportionately the orbital moment, which usually dominates the total uranium moment in compounds, and consequently the orbital moment was predicted to become comparable to the spin moment in UFe_2.

All the ferromagnetic uranium compounds studied, so far, by PND are characterized by a single U site in the crystallographic unit cell, both in the paramagnetic and the ferromagnetic states. The situation may be different for $U_4Ru_7Ge_6$. In the paramagnetic phase, $U_4Ru_7Ge_6$ crystallizes in the cubic Im-$3m$ space group with a single U site [20–22]. Our recent room-temperature XRPD measurement confirmed this statement [23]. Below $T_C = 10.7$ K, $U_4Ru_7Ge_6$ orders ferromagnetically with the ground state easy magnetization axis pointing along the [111] crystallographic axis. Thermal expansion measurements [23] show magnetostrictive effects of the order of 10^{-6}, and a subsequent rhombohedral distortion of the same order of magnitude. DFT calculations in the rhombohedral, ferromagnetic, ground state predict the splitting of the single cubic U site into two nonequivalent sites, with very different magnetic moments [23].

In this paper, we present a detailed PND study at low temperature on a single crystal, which provide microscopic experimental evidence of the aforementioned predictions. We also present further DFT calculations including the generalized gradient correction (GGA).

II. EXPERIMENTAL DETAILS

The $U_4Ru_7Ge_6$ single crystal used in this study was prepared by the Czochralski method in a tri-arc furnace. It was cut to $2 \times 2 \times 2\,mm^3$ cubic shape. Details of the growth and characterization are published elsewhere, as well as the room-temperature structure determination by x-ray powder diffraction (XRPD) on a powdered portion of the single crystal from the current study [23]. No sign of spurious phases has been detected either by XRPD nor by EDX analysis [23]. All the neutron scattering experiments were carried out at the ILL, Grenoble [24]. Polarized neutron diffraction was carried out using the D3 diffractometer. We collected a set of 448 flipping ratios up to $\frac{\sin\theta}{\lambda} = 0.7\,\text{Å}^{-1}$ with incident beam polarization of 0.95 and wavelength $\lambda = 0.85$ Å. To extract the magnetic structure factors from the polarized neutron data, one must have an accurate knowledge of the nuclear structure from the same sample at the same temperatures, including the extinction corrections. For a quick check, we used the Laue instrument CYCLOPS. A full unpolarized data collection was carried out at the D9 diffractometer. At each temperature, we collected a set of 1190 reflections with $0.1\,\text{Å}^{-1} < \frac{\sin\theta}{\lambda} < 1.0\,\text{Å}^{-1}$ using a wavelength of $\lambda = 0.841$ Å.

III. RESULTS

A. Structural study

The room-temperature space group Im-$3m$ has the group R-$3m$ as the only rhombohedral maximal subgroup [25]. In the frame of the R-$3m$ space group, a former single U site in a Wyckoff position $8c$ is split into two different sites U1 and U2 with Wyckoff position $3b$ and $9d$, respectively. As it is in agreement with the prediction of two different U sites with the same multiplicity by DFT [23], we assume R-$3m$ as a possible subgroup describing the ground-state structure of $U_4Ru_7Ge_6$. All the following data will be comparably refined using both the room temperature cubic space group Im-$3m$ and proposed distorted rhombohedral R-$3m$ space group, to rigorously study the ground-state structure. The transformations of the unit cell parameters, lattice vectors, atomic site fractional coordinates, and h,k,l indices between the Im-$3m$ and R-$3m$ space group are summarized in Table I, where we are using the hexagonal description of R-$3m$.

As can be seen from the lattice vector transformation in Table I, the rhombohedral R-$3m$ unit cell is rotated with respect to the cubic Im-$3m$ in the way that the former $[111]_{cub}$ direction is parallel with the new $[001]_{hex}$ and $[-110]_{cub}$ points along transformed $[100]_{hex}$ (see Fig. 1). The six $Ru2_{cubic}12d$ ions are forming a hexagonal arrangement around the U ions in the cubic structure that is perpendicular to the body diagonals. This local coordination is crucial for the structure of $U_4Ru_7Ge_6$, as the shortest interuranium distance $d_{U-U} = \frac{a_{cub}}{2} \approx 4.14665$ Å is rather large while the distance between U ion and the nearest Ru ions $d_{U-Ru2_{cubic}} \approx 2.93212$ Å highlights the importance of hybridization between U $5f$ and Ru $4d$ wave functions. The proposed symmetry change is most pronounced in the change of the fractional coordinate x of the $Ru2_{cubic}12d$ ($Ru2_{hex}\ 18g$) site, which is no longer fixed by symmetry. Formerly, the U position $8c$ has $.-3m$ point symmetry (it has no symmetry along the cubic primary directions in the $\{100\}_{cub}$ family, threefold rotoinversion axis along the secondary direction family $\{111\}_{cub}$ and mirror plane perpendicular to the $\{110\}_{cub}$ family). As the fractional coordinate x of the $Ru2_{hex}$ position starts to deviate from the 0.25 value, this strict hexagonal arrangement is conserved only for the U1 sites in the distorted rhombohedral structure. It can be seen from the preserved site symmetry of the U1 site, which is $-3m$ (primary direction of the rhombohedral lattice in the hexagonal axes is $\{001\}_{hex}$, which is in our case parallel with the $\{111\}_{cub}$, and secondary direction is $\{100\}_{hex}$, parallel with the $\{110\}_{cub}$), while the U2 site has only $.2/m$ symmetry and the hexagonal arrangement of the Ru ions is distorted. This distortion leads to the emergence of two different distances between U2 and $Ru2_{hex}$ sites. The first one depends only on the lattice parameter a_{hex} as $dU2 - Ru2_{hex,1} = a_{hex}\,(0.5 - x_{Ru2})$, while the second

TABLE I. Summary of the structural transformation between Im-3m and R-3m space group. Underlined coordinates in the R-3m space group are free parameters and are thus connected with the distortion.

Im-3m		R-3m, hexagonal axes	
U 8c	(0.25, 0.25, 0.25)	U1 3b U2 9d	(0, 0, 0.5) (0.5, 0, 0.5)
Ru1 2a	(0,0,0)	Ru1 3a	(0, 0, 0)
Ru2 12d	(0.25, 0, 0.5)	Ru2 18g	$(\underline{x_{\mathrm{Ru2}}}, 0, 0.5)$, $\underline{x_{\mathrm{Ru2}}} \sim 0.25$
Ge 12e	$(x_{\mathrm{Ge}}, 0, 0)$, $x_{\mathrm{Ge}} \sim 0.31$	Ge 18h	$(\underline{\frac{x_{\mathrm{Ge}}}{3}}, \underline{\frac{-x_{\mathrm{Ge}}}{3}}, \underline{\frac{-2x_{\mathrm{Ge}}}{3}})$
$a_{\mathrm{cub}}, V_{\mathrm{cub}}$		$\vec{a_{\mathrm{hex}}} = \vec{b_{\mathrm{cub}}} - \vec{a_{\mathrm{cub}}}$, $a_{\mathrm{hex}} = \sqrt{2}a_{\mathrm{cub}}$ $\vec{c_{\mathrm{hex}}} = \frac{1}{2}(\vec{a_{\mathrm{cub}}} + \vec{b_{\mathrm{cub}}} + \vec{c_{\mathrm{cub}}})$, $c_{\mathrm{hex}} = \frac{\sqrt{3}}{2}a_{\mathrm{cub}}$ $V_{\mathrm{hex}} = \frac{3}{2}V_{\mathrm{cub}}$	

$$(h,k,l)_{\mathrm{hex}} = (h,k,l)_{\mathrm{cub}} \begin{pmatrix} -1 & 0 & \frac{1}{2} \\ 1 & -1 & \frac{1}{2} \\ 0 & 1 & \frac{1}{2} \end{pmatrix}$$

one varies as $\mathrm{dU2} - \mathrm{Ru2}_{\mathrm{hex},2} = \sqrt{\frac{1}{48}a_{\mathrm{hex}}^2 + \frac{1}{9}c_{\mathrm{hex}}^2}$. The unique distance between U1 and $\mathrm{Ru2}_{\mathrm{hex}}$ is described in a similar way as $\mathrm{dU1} - \mathrm{Ru2}_{\mathrm{hex}} = a_{\mathrm{hex}}\, x_{\mathrm{Ru2}}$. It has an effect on the local coordination of the U1 and U2 sites. An example of the number of atoms around the U1 and U2 sites as a function of the radial distance is presented in Ref. [26]. It shows, that the U2 site has less regular local structure leading to reduced degeneracy of the mutual distances with other types of atoms.

One should notice that the proposed small distortion does not cause the appearance of any additional Bragg reflections within the experimental sensitivity of our experiments. It only introduces different rules for merging of the equivalent reflections. This was confirmed using the neutron Laue diffractometer CYCLOPS, where we did not observe any additional reflections down to 2 K. See Ref. [26] for the Laue pictures.

The unpolarized neutron diffraction experiment gives 371(216) inequivalent reflections assuming a R-3m (Im-3m) space group. The internal agreement factor of the equivalent reflections was 4.74% (6.43%) at 1.9 K and 3.50% (4.40%) at 20 K for R-3m (Im-3m) space group. It was thus always slightly better using the distorted R-3m space group, even in the paramagnetic phase.

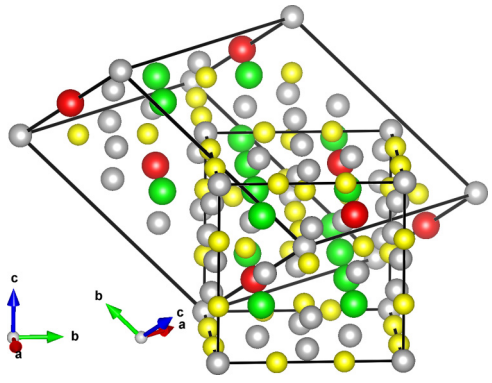

FIG. 1. Mutual orientation of the cubic Im-3m unit cell and the rhombohedral R-3m in the hexagonal axes. U1 sites are marked red, U2 green, Ru1 and Ru2 gray, and Ge are yellow.

As the intensities at 1.9 K (ordered state) should be affected both by nuclear and magnetic contribution, we have measured the temperature dependence of four different strong reflections from 15 K down to 1.9 K. Their intensity did not show any significant change. Such observation is acceptable since the spontaneous magnetic moment of $U_4Ru_7Ge_6$ is only $0.85\,\mu_B/f.u.$. We have also treated the reflections with a large enough scattering vector, i.e., $\frac{\sin\theta}{\lambda} > 0.6\,\mathrm{\AA}^{-1}$, separately. These should be much less affected by the magnetic contribution as was later confirmed by a polarized neutron experiment where reflections above this value showed flipping ratios close to 1 (see Sec. III C.).

The breaking of symmetry can lead to the existence of the twins (four types of the domains in our case). We have checked this possibility and refined our data with including these four twin components. However, based on the twin domain fractions obtained for each twin domain [97(2) : 0(2) : 0(1) : 3 %], we can conclude that after the phase transition, the sample remains mainly a single domain.

The structure was refined from the measured integrated intensities, corrected for absorption, using the FULLPROF software package [27,28], including extinction corrections and isotropic temperature factors B_{iso}. The B_{iso} parameter is proportional to the root mean square displacement of the atom from its average position. The results are summarized in Table II, with different agreement factors R_{F} for the cubic (Im-3m) and rhombohedral (R-3m) space groups. The crystallographic R_{F} factor is defined as a sum of the absolute values of differences between observed and calculated structure factors multiplied by 100 and divided by the sum of the absolute values of the observed structure factors. The negative isotropic temperature factor B_{iso} for a U ion at 1.9 K, when only reflections with $\frac{\sin\theta}{\lambda} > 0.6\,\mathrm{\AA}^{-1}$ are assumed, is consistent with our model of loss of the cubic symmetry in the ground state. Nevertheless, it can not be taken as a clear evidence for the structure change. A possible site mixing was also checked with no significant effect on the agreement factors. The crucial

TABLE II. Structural parameters and isotropic temperature factors B_{iso} obtained from the refinement of the neutron diffraction data, together with the corresponding agreement factors R_F. The rows labeled as 20 and 1.9 K show results for refinement using the whole set of reflections, while the one labeled as 1.9 K, $q > 0.6$ Å^{-1} shows results only for the reflections with $q > 0.6$ Å^{-1}.

	Im-3m						
	B_{iso}(Å^2)				x_{Ge}		R_F
	U		Ru1	Ru2	Ge		
20 K	0.075(12)		0.120(12)	0.130(27)	0.120(12)	0.3114(1)		3.72
1.9 K	0.066(12)		0.117(12)	0.127(28)	0.115(12)	0.3115(1)		3.66
1.9 K, $q > 0.6$ Å^{-1}	-0.049(10)		0.006(7)	0.020(13)	0.001(7)	0.3115(1)		3.05
	R-3m						
	B_{iso}(Å^2)						
	U1	U2	Ru1	Ru2	Ge	x_{Ge}	x_{Ru2}	R_F
20 K	0.060(23)	0.106(26)	0.090(10)	0.094(10)	0.039(12)	0.3117(2)	0.2500(1)	4.05
1.9 K	0.057(23)	0.031(12)	0.088(25)	0.096(10)	0.093(10)	0.3114(2)	0.2500(1)	3.98
1.9 K, $q > 0.6$ Å^{-1}	0.006(17)	0.016(11)	0.067(18)	0.045(10)	0.055(10)	0.3112(1)	0.2498(1)	3.32

importance of the performed neutron diffraction study was the structure determination as far as possible, including the extinction and absorption correction, on the same crystal and at the same temperature as in the following polarized neutron experiment.

B. DFT calculations

Details of our calculations can be found in our previous work [23]. To obtain the microscopic information about the values of spin and orbital magnetic moments, we applied the methods based on density functional theory (DFT). To solve Kohn-Sham-Dirac four-component equations, we used the latest version of the computer code full potential local orbitals (FPLO) [29]. We used several k meshes in the Brillouin zone to ensure the convergence of charge densities, total energy, and magnetic moments. For the sake of simplicity, we assume the ferromagnetic arrangement of the magnetic structure and the local spin density (LSDA) [30] within the generalized gradient approximation (GGA) [31] were used for the exchange and correlation contribution to the total energy. The 5f states of uranium were treated as itinerant Bloch states.

To further test the performance of LSDA and GGA, the equilibrium volume was calculated and compared with the experimental value V_0. The LSDA overbinds the minimal volume by 4.8 % ($V/V_0 = 95.2$). In contrast to this value, the GGA [31] improves the agreement with experiment remarkably ($V/V_0 = 1.01$). Therefore the GGA description [31] of $U_4Ru_7Ge_6$ seems to be more precise than LSDA [30]. The calculated components of the magnetic moment using GGA for all the atoms in the unit cell are listed in Table III.

C. Polarized neutron diffraction study

The flipping ratio method using a polarized neutron beam is a powerful tool to study small magnetic moments. It is based on the measurement of the flipping ratio $R = \frac{I^+}{I^-}$ of scattered intensities I^+ and I^-, with the primary beam polarized parallel (+) or antiparallel (−) to the applied vertical field direction. The magnetic easy axis of $U_4Ru_7Ge_6$ at the ground state is $[111]_{cub}$ (i.e., $[001]_{hex}$) [23]. Our sample was thus aligned to have the external vertical magnetic field parallel to that direction. We collected a set of flipping ratios at the same temperatures (1.9 and 20 K) as in the unpolarized experiment. The applied magnetic field was 1 and 9 T for both measured temperatures.

The obtained results were treated both with respect to cubic Im-3m and rhombohedral R-3m space group. While merging the equivalent flipping ratios obtained in 9 T and 1.9 K within the rhombohedral R-3m space group leads to the 78 independent values with internal agreement factor of 1%, the same approach for the cubic Im-3m space group gives 52 independent values with a degraded 3.5 % internal agreement factor. The inadequacy of the cubic description can be further illustrated by the example of the two reflections with dramatically different flipping ratios. These are namely $(030)_{hex}$ reflection with $R = 1.28(2)$ and $(211)_{hex}$ with $R = 0.79(2)$ as two inequivalent ones in the R-3m space group. But according to the Im-3m space group, they should be equivalent within the $\{2-11\}_{cub}$ family. It clearly shows that the cubic space group Im-3m cannot be used to describe the ground state of $U_4Ru_7Ge_6$. Same result were observed for the data obtained at 1.9 K in 1 T and at 20 K and 9 T. We will thus focus only on the description using the rhombohedral R-3m space group in the following treatment of polarized neutron data, both using maximum entropy calculations or direct flipping ratios refinement.

1. Maximum entropy method (MAXENT)

The maximum entropy approach is not affected by any prior assumption of the distribution of magnetic density. Its only inputs are the symmetry and dimensions of the unit cell and the magnetic structure factors obtained from the measured flipping ratios. In our case, the whole unit cell was divided into 235 × 235 × 145 separated voxels. We used DYSNOMIA software utilizing the CAMBRIDGE algorithm [32] to calculate the most probable spin density map. The initial state was a flat magnetic density distribution over the unit cell. The results are plotted using the VESTA software [33]. The resulting three-dimensional spin density map agrees with the experimental magnetic structure factors and has maximal

TABLE III. Magnetic moments calculated from DFT, obtained by MAXENT and from the direct fitting of the flipping ratios using dipolar approximation in 1 T and 9 T at 1.9 K and 20 K. All values are in the μ_B.

	DFT		MAXENT			Dipolar approximation					
	GGA		1 T, 1.9 K	9 T, 1.9 K	9 T, 20 K	1 T, 1.9 K $\chi^2 = 1.27$		9 T, 1.9 K $\chi^2 = 1.49$		9 T, 20 K $\chi^2 = 1.02$	
Atom, mult.	μ_S μ_L	μ	μ	μ	μ	μ_S μ_L	μ	μ_S μ_L	μ	μ_S μ_L	μ
U1, 1	−0.657 0.554	−0.103	0.11(1)	0.17(1)	0.10(1)	0.17(4) −0.04	0.129(9)	0.23(5) −0.05	0.18(1)	0.15(4) −0.02(4)	0.13(1)
U2, 3	−0.820 1.021	0.201	0.16(1)	0.22(1)	0.14(1)	−0.26(2) 0.43(2)	0.176(6)	−0.28(3) 0.51(2)	0.230(8)	−0.26(2) 0.43(2)	0.172(6)
Ru1, 1	−0.110 −0.005	−0.115	–	–	–	0.04(4) −0.03(4)	0.01(1)	0.00(5) 0.00(4)	0.00(2)	0.00(4) 0.004	0.00(1)
Ru2, 6	0.119 0.009	0.128	–	–	–	0.07(2) −0.05(2)	0.021(5)	0.11(2) −0.08(2)	0.030(6)	0.09(1) −0.07(1)	0.024(4)
Ge, 6	0.009 0.004	0.013	–	–	–	– –	–	– –	–	– –	–
μ_{sum}		1.231	0.85(2)	1.05(2)	0.84(2)		0.79(4)		1.02(4)		0.79(4)
μ_{bulk}			0.94(1)	1.25(1)	0.98(1)		0.94(1)		1.25(1)		0.98(1)

entropy. Figure 2 shows the spin density map obtained at 9 T and 1.9 K in a slice perpendicular to the $[001]_{hex}$ axis at the fractional coordinate $z \approx 0.833333$. This slice truncates both the U1 and U2 ions and evidences a density almost three times higher on the U2 sites than on the U1 site: ∼0.24 and ∼0.078 μ_B Å^{-3}, respectively, at the center. Integration in the spherical region around the given atomic position can serve as a rough estimation of the magnetic moments associated to each site. We have performed integration in the sphere with gradually increasing radius. The obtained magnetic moments showed saturation around ∼1.8 Å for both the U1 and U2 positions. This value is close to the experimental atomic radius of 1.75 Å of uranium [34]. See Ref. [26] for the integrated magnetic moment as a function of the radius. Integrated values are 0.17(1) μ_B and 0.22(1) μ_B for the U1 and U2 site at 9 T and 1.9 K, respectively. Qualitatively comparable results were obtained for the measurement at 1.9 K and 1 T and at 20 K, and 9 T. See Ref. [26] for the corresponding magnetization density maps. All values are summarized in Table III.

2. *Direct refinement of the flipping ratios*

To describe the magnetic structure of $U_4Ru_7Ge_6$ in more detail and distinguish between the spin μ_S and orbital μ_L components of the magnetic moments, we compared the measured flipping ratios (or magnetic structure factors) with a model, in the dipolar approximation. Our least squares refinement was performed using the FULLPROF/WINPLOTR [27,28] software. The dipolar approximation uses an isotropic description of the magnetic form factors $f_M(q)$ and can be written as

$$f_M(q) = \mu(\langle j_0(q)\rangle + C_2\langle j_2(q)\rangle),$$
$$C_2 = \frac{\mu_L}{\mu} = \frac{\mu_L}{\mu_L + \mu_S}, \quad (1)$$

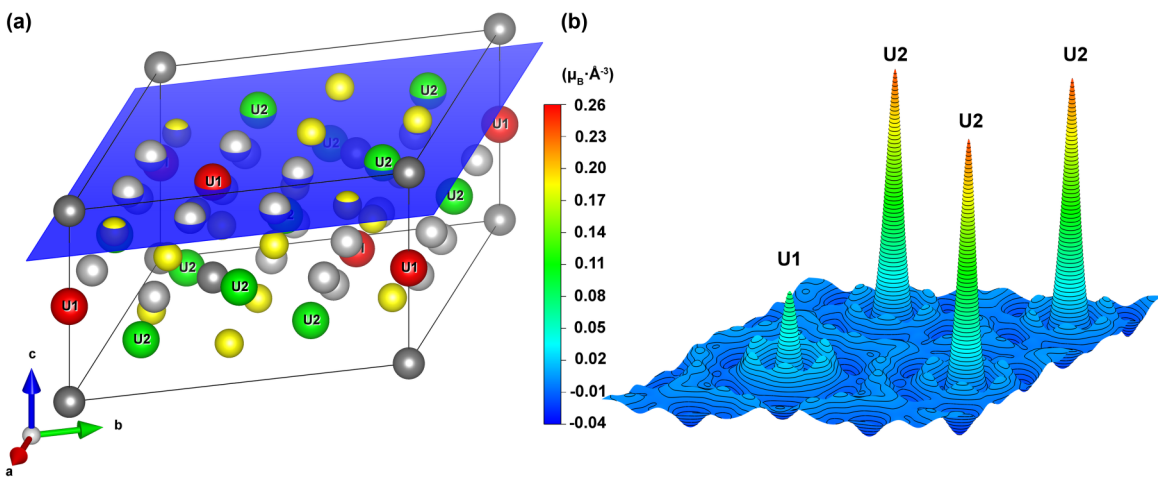

FIG. 2. (a) Indicated section in the *R*-3*m* space group representation that is perpendicular to the $[001]_{hex}$ axis, and (b) the corresponding MAXENT magnetization density map measured in 9 T and 1.9 K. Contour lines are at 0.004 μ_B Å^{-3}.

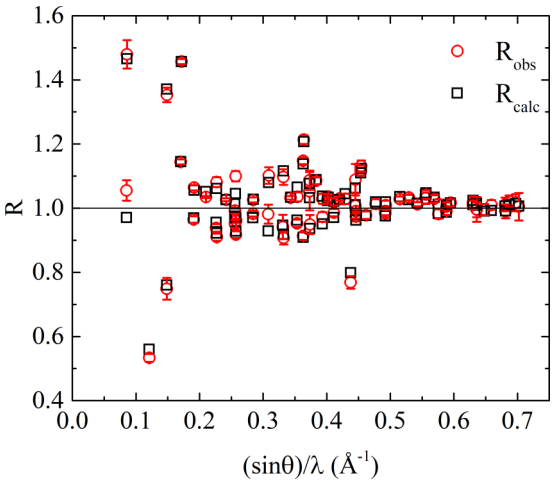

FIG. 3. Flipping ratios measured at 1.9 K and 9 T compared with the calculated values using the dipolar approximation.

where $\langle j_0(q)\rangle$ and $\langle j_2(q)\rangle$ are the expectation values of the spherical Bessel functions. These are approximated by the series of exponential functions with proper coefficients [35]. Using these tabulated values, we can extract the spin μ_S and orbital μ_L magnetic moments. We used the Ru^{1+} values for ruthenium and either the U^{3+} or the U^{4+} values for uranium (although the actual valence of uranium in $U_4Ru_7Ge_6$ may be different).

The assumed ground-state space group R-3m of $U_4Ru_7Ge_6$ has two different U and Ru sites but, according to the symmetry, every $f_M(q_{h,k,l})$ reflection has a contribution from all four sites, and one has to include them all at once into the least squares fit. Best fits for all experimental conditions were obtained assuming a U^{3+} form factor, although the difference between U^{3+} and U^{4+} form factor is very small [36]. The results are summarized in Table III. As an example, the measured and calculated flipping ratios are plotted in Fig. 3 for the (9 T, 1.9 K) data set. See Ref. [26] for the comparison of the measured and calculated flipping ratios for the measurements at 1.9 K and 1 T and at 20 K and 9 T [26].

We first discuss the results in the ordered state. The spin and orbital moments on the U2 site are antiparallel with a dominant orbital contribution leading to a ratio of $\frac{\mu_L}{\mu_S} = -1.7(2)$ $[-1.8(2)]$ and parameter C_2 reaches a value of 2.5(1) [2.3(1)] at 1 T [9 T].

The orbital component of the magnetic moment on the U1 site is very small: $-0.04(4)\,\mu_B$ and $-0.05(4)\,\mu_B$ at 1 T and 9 T, respectively. Together with the dominating spin component it gives a very unusual value of the ratio of $\frac{\mu_L}{\mu_S} = -0.2(2)$ $[-0.2(2)]$ and a very small and negative parameter $C_2 = -0.3(3)$ $[-0.3(2)]$.

The resulting magnetic moment on the Ru1 position is negligible both in 1 T and 9 T. On the other hand, the Ru2 position shows a clear induced moment $[0.021(5)\,\mu_B$ and $0.030(6)\,\mu_B$ for 1 and 9 T, respectively$]$.

The bulk magnetization value μ_{bulk} resulting from the magnetometry measurements increases by a factor 1.3 between 1 T $[0.94(1)\,\mu_B]$ and 9 T $[1.25(1)\,\mu_B]$ [23]. This scaling is valid within the experimental error, for all the fitted magnetic moments of the U and Ru ions. The resulting total magnetic moments per formula unit, $\mu_{sum} = \mu_{U1} + 3\mu_{U2} + \mu_{Ru1} + 6\mu_{Ru2}$, are $0.79(4)\,\mu_B$ and $1.02(4)\,\mu_B$ for 1 T and 9 T, respectively, smaller than the bulk magnetization values. The residual moment $\mu_{res} = \mu_{bulk} - \mu_{sum}$ can be attributed to the polarization of the conduction electrons. Due to the large spatial extent of the conduction electrons, their form factor vanishes around $\frac{\sin\theta}{\lambda} = 0.1\,\text{Å}^{-1}$ [37] and cannot be observed in our neutron diffraction experiments. This μ_{res} value is $0.15(4)\,\mu_B$ and $0.23(4)\,\mu_B$ for 1 T and 9 T, respectively, reaching ~17% of the bulk magnetic moment for both cases.

The bulk magnetic moment above the ordering temperature at 20 K, induced by the external magnetic field of 9 T, is $0.98(1)\,\mu_B$. This value is close to the moment in the ordered state at 1.9 K in the field of 1 T, which reaches the value of $0.94(1)\,\mu_B$. The analysis of the flipping ratios obtained in these conditions, i.e., above T_C, at 20 K and 9 T, gives comparable results to those obtained at 1.9 K and 1 T, i.e., the U1 and U2 position shows remarkably different magnetic moments. Results of the fit are summarized in Table III. All the components of magnetic moments on all the U and Ru sites are almost equal within the experimental error.

IV. DISCUSSION

Using unpolarized neutron single crystal diffraction methods is not sufficient to undoubtedly solve the ground-state structure of the system, as the proposed distortion of the cubic structure is very small (in the order of 10^{-6}). Comparison of the agreement factors R_F for the Im-3m and R-3m space groups actually favors the cubic structure both in the ordered state and above T_C (see Table II). However, this may be biased by the fact that the number of inequivalent reflections is much higher for the rhombohedral structure, and the internal agreement factor for the equivalent reflections was always worse for the cubic structure model. The value of the fractional coordinate $x_{Ru2_{hex}}$, which is not fixed in the distorted structure, is close to the value of 0.25 given by symmetry in the cubic description, for both the measurements at 20 K and 1.9 K. It thus keeps the dU1-$Ru2_{hex}$ and dU2-$Ru2_{hex,1}$ distances almost equal and the largest effect of the interatomic distance change can be expected for dU2-$Ru2_{hex,2}$ that is controlled only by the change of the lattice parameters a_{hex} and c_{hex}. This variation of the lattice parameters was revealed as a strong evidence for the distortion observed by our previous precision measurement of the thermal expansion [23]. Further proof is brought by the polarized neutron study, which clearly evidences two uranium sites with drastically different magnetic moments. Further detailed structural study of this compound, like high resolution x-ray diffraction, is desired.

The first-principles calculations presented in our previous work [23] and further improved in this paper clearly show the necessity to incorporate the spin-orbit interaction while treating the uranium-based intermetallics. Previous calculations of magnetic moments performed on the $U_4Ru_7Ge_6$ omitted the relativistic effects [38]. This spin only approach naturally deals with only one U position as the lack of spin-orbit interaction does not lower the symmetry. It gives a total magnetic moment of $\sim 2.72\,\mu_B/f.u.$ that overestimates the experimental bulk value. Our results using GGA give a total magnetic moment of

$\sim$1.23 $\mu_B/f.u.$, much closer to the bulk magnetization value ($\sim$1.25 $\mu_B/f.u.$ at 1.9 K and 9 T). The spin-orbit interaction also leads to the appearance of two distinct U sites (U1 and U2), in agreement with our proposed rhombohedral distortion. Our DFT calculations show antiparallel alignment of the spin and orbital magnetic moments both on the U1 and U2 sites (see Table III). This is expected from the third Hund's rule [39] for systems with less than half-filled shells. The spin moments on the U1 and U2 sites are parallel. However, the total magnetic moment of the U1 site is expected to be dominated by its spin component, leading to a mutually antiparallel alignment of the U1 and U2 total moments and resulting in a ferrimagnetic structure in the ground state of $U_4Ru_7Ge_6$. Such a behavior was observed by neutron powder diffraction in the case of UCu_5Sn where two different U sites possess antiparallel collinear magnetic moments of dramatically different magnitudes of 2.14(2) $\mu_B/f.u.$ on the 2a and 0.18(4) $\mu_B/f.u.$ on the 2c position [40]. It is believed to be caused by Kondo screening, acting strongly on the 2c position. Availability of only unpolarized neutron data prevented the authors from distinguishing between the spin and orbital components.

Our polarized neutron diffraction results are in good qualitative agreement with the DFT calculations and gives independent and clear experimental evidence of the presence of two different U sites, excluding the cubic Im-3m space group as a proper ground-state structure. However, while both the maximum entropy calculations and a direct fit of the flipping ratios clearly show a different density of magnetic moments on the U1 and U2 sites, they also reveal a positive magnetic moment on both of them, in disagreement with the DFT calculations (see Table III).

Our refined model for fitting of flipping ratios gives a rather large $C_2 \sim 2.5$ parameter, irrespective of the applied magnetic field, for the U2 site. It is much higher than the theoretical values calculated within the intermediate coupling scheme for the free U^{3+} (1.64) and U^{4+} (1.43) ions. These correspond to a ratio $\frac{\mu_L}{\mu_S}$ of -2.55 and -3.34 for U^{3+} and U^{4+}, respectively [41]. The U2 site exhibits $\frac{\mu_L}{\mu_S} \sim -1.7$ independent of the applied field. This ratio depends very strongly on the degree of hybridization between the uranium 5f and transition-metal d wave functions and its decrease from the free ion values means strengthening of the hybridization [42]. In that sense, the 5f wave function of the U2 ion strongly hybridizes with the surrounding Ru 4d-wave functions as expected from its coordination. Similar values of the C_2 parameter can be found in the case of antiferromagnetic compounds $UNiGa_5$ [43] [2.45(7)] and UGa_3 [44] [2.52(5)].

The total U1 magnetic moment, obtained from polarized neutrons is opposite to the DFT prediction. It also has an extremely small orbital moment irrespective of the applied magnetic field. This means an almost quenched orbital moment of the U ion on the U1 position, which is quite surprising and unexpected. Similar effects were already observed only in the case of metallic α-uranium, for which the measured magnetic form factor can be approximated as spin-only and varies significantly from the one usually observed for the uranium-based compounds [45]. A later theoretical study actually describes α-uranium as a system where the third Hund's rule is not valid and the orbital moment can be parallel to the spin moment [46,47].

Our DFT calculations of $U_4Ru_7Ge_6$ also predict non-negligible induced moments on both the Ru sites. They are expected to be antiparallel to each other with dominating spin components. A small magnetic moment is also predicted to be present on the Ge site. In disagreement with the DFT calculations we found only negligible magnetic moment on the Ru1 site. On the other hand, the Ru2 site exhibits a significant induced moment dominated by its spin component. These Ru2 ions form a hexagonal arrangement around the U1 site and a distorted hexagon around the U2 position. The ratio of the magnetic moment on the Ru2 site and the U2 site is $\approx$0.12 both at 1 T and 9 T and $\approx$0.16 for the U1 site. This is another direct evidence for the hybridization between U 5f and Ru 4d wave functions. This resembles the case of URuAl, where the ratio of the Ru induced magnetic moment to the U moment is even bigger, 0.45(8) [48]. Parallel alignment of the magnetic moment on the U2 and the Ru2 sites can be understood by analogy with the mechanism proposed by Brooks *et al.* [49]. This was used to describe the parallel orientation of the moment on the U and the Co sites in UCoGe observed by XMCD [50], although polarized neutron diffraction showed an antiparallel arrangement [51]. According to that, we would expect our 4d spins of Ru to be antiferromagnetically coupled to the 6d spins of U. Thanks to a positive intra-atomic Hund's rule exchange, these U 6d spin moments are coupled parallel to the 5f spin moments. Antiferromagnetic coupling of spin and orbital components on U then results in a final parallel orientation of the Ru and U moments.

The GGA DFT magnetic moments are only in semiquantitative agreement with the experimental results obtained by the MAXENT method and dipolar approximation including the fitting of form factors. One should take into account that the GGA results were obtained at zero magnetic field whereas the magnetic fields of 1 T and 9 T were applied in experiment. Therefore the GGA calculations can be taken as the first approximation to the complex ferromagnetic ground state of $U_4Ru_7Ge_6$ compound. For instance, the difference in the charge state of U1 and U2 atoms is only 0.002 electrons in GGA calculations. The difference in the charge state and the degree of the 5f(U) and 4d(Ru) hybridization between the U1 and U2 split states can be only roughly obtained using DFT GGA calculations. This points to future use of more a complex theory like, for example, dynamical mean-field theory (see, for instance, Ref. [52]), which is able to take into account the magnetic fluctuations at the U1 and U2 site. However, this is beyond the scope of the present, mainly experimental paper.

The residual moment in the unit cell μ_{res} is estimated to represent $\sim$17% of the bulk moment. A comparably large and positive (12%) value was observed in antiferromagnetic UPd_2Al_3 where it was attributed to the possible contribution of the outer Pd electrons, as there is no observed induced moment on the Pd site itself [37]. This compound has a similar coordination of U ions surrounded by hexagons of 4d ions as $U_4Ru_7Ge_6$ but at a larger distance of 3.12 Å. An even larger moment of μ_{res} was found in the uranium-based superconductor UCoGe, where it reaches 54%–85% of the bulk magnetic moment [51], depending on the used method.

The fact that we have observed different magnetic moments on U1 and U2 even in the paramagnetic state at 20 K in a 9 T applied field clearly shows that the proposed distortion

to the rhombohedral structure with two different U sites can also be induced by an external magnetic field even above the ordering temperature. The $\frac{\mu_L}{\mu_S}$ ratio remains unchanged relative to the ordered state, showing that there is no change in the nature of the $5f$ wave functions between the ferromagnetic and paramagnetic state. Similar results were found in the case of ferromagnetic superconductor UGe_2 [53].

It has to be noticed that we assumed only a colinear (z component) alignment of the magnetic moments in our study. If we take the R-3m space group as the real ground state structure and assume U1, U2, Ru1, and Ru2 as the only positions with magnetic moments, then there are four possible maximal magnetic space groups for the propagation vector (0,0,0) (i.e., a ferromagnetic state). Among these R-3m' is the only one that allows moment on all these four positions [25]. In the most general case, it allows a magnetic component out of the z direction on the U2 and Ru2 position.

Only very few uranium based systems with two different U sites have been studied by neutrons. A ferrimagnetic ground state was confirmed for the above mentioned UCu_5Sn [40]. Burlet *et al.* [54] describes the antiferromagnetic order of the $U_4Cu_4P_7$ with two different U sites as a result of their different valence states. We are unable to make any conclusions regarding the valence of U ions in the case of $U_4Ru_7Ge_6$, since the U^{3+} and U^{4+} form factors are very similar and we also expect a rather itinerant nature of the ferromagnetism. Nevertheless, to our knowledge, $U_4Ru_7Ge_6$ is so far the only uranium based ferromagnet that shows a structural distortion in the ordered state, connected with the appearance of two different, formerly symmetry equivalent, U sites.

From the point of view of correct determination of form factors of dramatically reduced $5f$-electron magnetic moments and their orbital and spin components by neutron diffraction, $U_4Ru_7Ge_6$ represents an extremely difficult case for several reasons, mainly: (i) two inequivalent U sites/magnetic moments, (ii) lack of reflections arising from only one of U sites, and (iii) non-negligible Ru 4d-electron induced moments. Microscopic site-selective experiments are strongly desired for further progress in understanding the physics of this unique U intermetallic compound. Considering the strongly reduced U magnetic moments, valuable information may be expected from a complex μSR study including determination of the possible muon stopping site(s).

V. CONCLUSIONS

We have presented experimental evidence of a distortion of the $U_4Ru_7Ge_6$ cubic lattice in the ferromagnetic state, which was predicted by DFT calculations and thermal expansion measurements. This transition from the Im-3m space group to a lower symmetry, most probably described by R-3m space group, is caused by the dramatic influence of the spin-orbit interaction on the local symmetry of the U ion site. It results in the emergence of two crystallographically inequivalent U sites, U1 and U2, with remarkably different magnetic moments. We have shown that this effect cannot be observed by usual (unpolarized) neutron diffraction, but it appears clearly in our polarized neutron diffraction data. Results of the maximum entropy calculations together with a model based on the dipolar approximation undoubtedly show the presence of distinct U1 and U2 sites not only in the ground state of the compound, but also in the magnetic field (applied along the easy [111] direction) induced state in the paramagnetic regime. Our data suggest a direct connection of the distortion with the magnetic structure, even when it is field induced in the paramagnetic state. The large value of the $C_2 \sim 2.5$ parameter of the U2 position suggests an important role of the hybridization of $5f$ orbitals with the surrounding Ru 4d wave functions and is far from the theoretical values of the U^{3+} or U^{4+} free ions. Refinement of our data points toward an almost quenched orbital moment on the U1 site. $U_4Ru_7Ge_6$ also exhibits a magnetic moment on the Ru2 position corroborating the strong hybridization of the $5f$ U and 4d Ru wave functions.

ACKNOWLEDGMENTS

The work was supported within the program of Large Infrastructures for Research, Experimental Development and Innovation (Project No. LM2015050) and project LTT17019 financed by the Ministry of Education, Youth and Sports, Czech Republic. This work was supported by the Czech Science Foundation Grant No. 16-06422S. Experiments were performed in the Materials Growth and Measurement Laboratory MGML (see: http://mgml.eu/). The authors are indebted to Ross H. Colman for reading the manuscript and providing language corrections.

[1] M. S. S. Brooks and P. J. Kelly, Phys. Rev. Lett. **51**, 1708 (1983).
[2] M. S. S. Brooks, Physica B+C **130**, 6 (1985).
[3] O. Eriksson, M. S. S. Brooks, and B. Johansson, Phys. Rev. B **41**, 9087 (1990).
[4] O. Eriksson, M. S. S. Brooks, and B. Johansson, Phys. Rev. B **41**, 7311 (1990).
[5] L. Severin, L. Nordström, M. S. S. Brooks, and B. Johansson, Phys. Rev. B **44**, 9392 (1991).
[6] M. R. Norman and D. D. Koelling, Phys. Rev. B **33**, 3803 (1986).
[7] M. R. Norman, B. I. Min, T. Oguchi, and A. J. Freeman, Phys. Rev. B **38**, 6818 (1988).
[8] F. A. Wedgewood and M. Kuzneitz, J. Phys. C **5**, 3012 (1972).
[9] G. H. Lander, J. Faber, A. J. Freeman, and J. P. Desclaux, Phys. Rev. B **13**, 1177 (1976).
[10] J. Faber and G. H. Lander, Phys. Rev. B **14**, 1151 (1976).
[11] G. H. Lander, M. H. Mueller, D. M. Sparlin, and O. Vogt, Phys. Rev. B **14**, 5035 (1976).
[12] A. Delapalme, G. H. Lander, and P. J. Brown, J. Phys. C **11**, 1441 (1978).
[13] D. D. Koelling, B. D. Dunlap, and G. W. Crabtree, Phys. Rev. B **31**, 4966 (1985).
[14] O. Eriksson, B. Johansson, M. S. S. Brooks, and H. L. Skriver, Phys. Rev. B **40**, 9508 (1989).
[15] V. Sechovský, Z. Smetana, G. Hilscher, E. Gratz, and H. Sassik, Physica B+C **102**, 277 (1980).

[16] J. M. Fournier, A. Boeuf, P. Frings, M. Bonnet, J. v. Boucherle, A. Delapalme, and A. Menovsky, J. Less-Common Met. **121**, 249 (1986).

[17] M. Wulff, G. H. Lander, B. Lebech, and A. Delapalme, Phys. Rev. B **39**, 4719 (1989).

[18] B. Lebech, M. Wulff, and G. H. Lander, J. Appl. Phys. **69**, 5891 (1991).

[19] M. S. S. Brooks, O. Eriksson, B. Johansson, J. J. M. Franse, and P. H. Frings, J. Phys. F **18**, L33 (1988).

[20] A. A. Menovsky, J. Magn. Magn. Mater. **76-77**, 631 (1988).

[21] B. Lloret, B. Buffat, B. Chevalier, and J. Etourneau, J. Magn. Magn. Mater. **67**, 232 (1987).

[22] S. A. M. Mentink, G. J. Nieuwenhuys, A. A. Menovsky, and J. A. Mydosh, J. Appl. Phys. **69**, 5484 (1991).

[23] M. Vališka, M. Diviš, and V. Sechovský, Phys. Rev. B **95**, 085142 (2017).

[24] M. Vališka, O. R. Fabelo Rosa, M. Klicpera, V. Sechovský, and A. Stunault (2016), doi:10.5291/ILL-DATA.5-51-516

[25] M. I. Aroyo, J. M. Perez-Mato, C. Capillas, E. Kroumova, S. Ivantchev, G. Madariaga, A. Kirov, and H. Wondratschek, Z. Kristallogr. - Cryst. Mater. **221**, 15 (2006).

[26] See Supplemental Material at http://link.aps.org/supplemental/10.1103/PhysRevB.97.125128 for the detailed information about the data treatment.

[27] T. Roisnel and J. Rodriguez-Carvajal, in *EPDIC 7 - Seventh European Powder Diffraction Conference*, edited by R. Delhez and E. Mittemeijer (Trans Tech Publications, 2000).

[28] J. Rodriguez-Carvajal, Physica B **192**, 55 (1993).

[29] K. Koepernik and H. Eschrig, Phys. Rev. B **59**, 1743 (1999).

[30] J. P. Perdew and Y. Wang, Phys. Rev. B **45**, 13244 (1992).

[31] J. P. Perdew, K. Burke, and M. Ernzerhof, Phys. Rev. Lett. **77**, 3865 (1996).

[32] K. Momma, T. Ikeda, A. A. Belik, and F. Izumi, Powder Diffr. **28**, 184 (2013).

[33] K. Momma and F. Izumi, J. Appl. Crystallogr. **44**, 1272 (2011).

[34] J. C. Slater, J. Chem. Phys. **41**, 3199 (1964).

[35] P. J. Brown, in *International Tables for Crystallography*, edited by E. Prince (Wiley, 2006), Vol. C, Sec. 4.4, pp. 454–461.

[36] A. J. Freeman, J. P. Desclaux, G. H. Lander, and J. Faber, Phys. Rev. B **13**, 1168 (1976).

[37] L. Paolasini, J. Paixao, G. H. Lander, A. Delapalme, N. Sato, and T. Komatsubara, J. Phys.: Condens. Matter **5**, 8905 (1993).

[38] S. F. Matar, B. Chevalier, and R. Pöttgen, Solid State Sci. **27**, 5 (2014).

[39] N. Ashcroft and N. Mermin, *Solid State Physics* (Saunders College, 1976), Sec. 31.

[40] V. H. Tran, R. Troc, G. André, F. Bourée, and M. Kolenda, J. Phys.: Condens. Matter **12**, 5879 (2000).

[41] G. van der Laan and B. T. Thole, Phys. Rev. B **53**, 14458 (1996).

[42] G. H. Lander, M. S. S. Brooks, and B. Johansson, Phys. Rev. B **43**, 13672 (1991).

[43] K. Kaneko, N. Metoki, N. Bernhoeft, G. H. Lander, Y. Ishii, S. Ikeda, Y. Tokiwa, Y. Haga, and Y. Onuki, Phys. Rev. B **68**, 214419 (2003).

[44] A. Hiess, F. Boudarot, S. Coad, P. J. Brown, P. Burlet, G. H. Lander, M. S. S. Brooks, D. Kaczorowski, A. Czopnik, and R. Troc, Europhys. Lett. **55**, 267 (2001).

[45] R. C. Maglic, G. H. Lander, M. H. Mueller, and R. Kleb, Phys. Rev. B **17**, 308 (1978).

[46] A. Hjelm, O. Eriksson, and B. Johansson, Phys. Rev. Lett. **71**, 1459 (1993).

[47] A. Hjelm, J. Trygg, O. Eriksson, B. Johansson, and J. Wills, Phys. Rev. B **50**, 4332 (1994).

[48] J. A. Paixão, G. H. Lander, A. Delapalme, H. Nakotte, F. R. d. Boer, and E. Brück, EPL (Europhysics Letters) **24**, 607 (1993).

[49] M. S. S. Brooks, O. Eriksson, and B. Johansson, J. Phys.: Condens. Matter **1**, 5861 (1989).

[50] M. Taupin, J. P. Sanchez, J. P. Brison, D. Aoki, G. Lapertot, F. Wilhelm, and A. Rogalev, Phys. Rev. B **92**, 035124 (2015).

[51] K. Prokeš, A. de Visser, Y. K. Huang, B. Fåk, and E. Ressouche, Phys. Rev. B **81**, 180407 (2010).

[52] A. Hariki, A. Hausoel, G. Sangiovanni, and J. Kuneš, Phys. Rev. B **96**, 155135 (2017).

[53] N. Kernavanois, B. Grenier, A. Huxley, E. Ressouche, J. P. Sanchez, and J. Flouquet, Phys. Rev. B **64**, 174509 (2001).

[54] P. Burlet, R. Troc, D. Kaczorowski, H. Noël, and J. Rossat-Mignod, J. Magn. Magn. Mater. **130**, 237 (1994).